Nonlinear photoacoustic microscopy via a loss modulation technique: from detection to imaging

Yu-Hung Lai,[1,2] Szu-Yu Lee[1], Chieh-Feng Chang,[1] Yu-Hsiang Cheng[1] and Chi-Kuang Sun[1,3,4,*]

[1]*Department of Electrical Engineering and Graduate Institute of Photonics and Optoelectronics, National Taiwan University, Taipei 10617, Taiwan*
[2]*Applied Physics Option, California Institute of Technology, Pasadena, California 91125, USA*
[3]*Institute of Physics and Research Center for Applied Sciences, Academia Sinica, Taipei 115, Taiwan*
[4]*Molecular Imaging Center and Graduate Institute of Biomedical Electronics and Bioinformatics, National Taiwan University, Taipei 10617, Taiwan*
[*]*sun@ntu.edu.tw*

Abstract: In order to achieve high-resolution deep-tissue imaging, multi-photon fluorescence microscopy and photoacoustic tomography had been proposed in the past two decades. However, combining the advantages of these two imaging systems to achieve optical-spatial resolution with an ultrasonic-penetration depth is still a field with challenges. In this paper, we investigate the detection of the two-photon photoacoustic ultrasound, and first demonstrate background-free two-photon photoacoustic imaging in a phantom sample. To generate the background-free two-photon photoacoustic signals, we used a high-repetition rate femtosecond laser to induce narrowband excitation. Combining a loss modulation technique, we successfully created a beating on the light intensity, which not only provides pure sinusoidal modulation, but also ensures the spectrum sensitivity and frequency selectivity. By using the lock-in detection, the power dependency experiment validates our methodology to frequency-select the source of the nonlinearity. This ensures our capability of measuring the background-free two-photon photoacoustic waves by detecting the 2nd order beating signal directly. Furthermore, by mixing the nanoparticles and fluorescence dyes as contrast agents, the two-photon photoacoustic signal was found to be enhanced and detected. In the end, we demonstrate subsurface two-photon photoacoustic bio-imaging based on the optical scanning mechanism inside phantom samples.

OCIS codes: (110.0110) Imaging systems; (110.0180) Microscopy; (180.4315) Nonlinear microscopy; (190.4180) Multiphoton processes; (110.5120) Photoacoustic imaging; (190.7110) Ultrafast nonlinear optics.

References and links

1. M. Rumi and J. W. Perry, "Two-photon absorption: an overview of measurements and principles," Adv. Opt. Photonics **2**(4), 451–518 (2010).
2. F. Helmchen and W. Denk, "Deep tissue two-photon microscopy," Nat. Methods **2**(12), 932–940 (2005).
3. L. V. Wang and S. Hu, "Photoacoustic tomography: In Vivo imaging from organelles to organs," Science **335**(6075), 1458–1462 (2012).
4. V. Ntziachristos, "Going deeper than microscopy: the optical imaging frontier in biology," Nat. Methods **7**(8), 603–614 (2010).
5. H. F. Zhang, K. Maslov, G. Stoica, and L. V. Wang, "Functional photoacoustic microscopy for high-resolution and noninvasive in vivo imaging," Nat. Biotechnol. **24**(7), 848–851 (2006).
6. Y. Yamaoka, M. Nambu, and T. Takamatsu, "Fine depth resolution of two-photon absorption-induced photoacoustic microscopy using low-frequency bandpass filtering," Opt. Express **19**(14), 13365–13377 (2011).
7. Y. Yamaoka, M. Nambub, and T. Takamatsu, "Frequency-selective multiphoton-excitation-induced photoacoustic microscopy (MEPAM) to visualize the cross sections of dense objects," Proc. SPIE 7564, 1–9 (2010).
8. N. Chandrasekharan, B. Gonzales, and B. M. Cullum, "Non-resonant Multiphoton Photoacoustic Spectroscopy for Noninvasive Subsurface Chemical Diagnostics," Appl. Spectrosc. **58**(11), 1325–1333 (2004).

#199491 - $15.00 USD Received 16 Oct 2013; revised 9 Dec 2013; accepted 9 Dec 2013; published 3 Jan 2014

9. M.E. van Raaij, M. Lee, E. Cherin, B. Stefanovic, and F.S. Foster, "Femtosecond photoacoustics: integrated two-photon fluorescence and photoacoustic microscopy," Proc. SPIE. 7564, 1-6 (2010).
10. G. Langer, K. D. Bouchal, H. Grün, P. Burgholzer, and T. Berer, "Two-photon absorption-induced photoacoustic imaging of Rhodamine B dyed polyethylene spheres using a femtosecond laser," Opt. Express **21**(19), 22410–22422 (2013).
11. S. Dahal, J. B. Kiser, and B. M. Cullum, "Depth and resolution characterization of two-photon photoacoustic spectroscopy for noninvasive subsurface chemical diagnostics," Proc. SPIE 8025, 1–7 (2011).
12. W. R. Zipfel, R. M. Williams, and W. W. Webb, "Nonlinear magic: multiphoton microscopy in the biosciences," Nat. Biotechnol. **21**(11), 1369–1377 (2003).
13. B. Huang, M. Bates, and X. Zhuang, "Super-Resolution Fluorescence Microscopy," Annu. Rev. Biochem. **78**(1), 993–1016 (2009).
14. P. Tian and W. S. Warren, "Ultrafast measurement of two-photon absorption by loss modulation," Opt. Lett. **27**(18), 1634–1636 (2002).
15. R. L. Shelton and B. E. Applegate, "Ultrahigh resolution photoacoustic microscopy via transient absorption," Biomed. Opt. Express **1**(2), 676–686 (2010).
16. M. Xu and L. V. Wang, "Photoacoustic imaging in biomedicine," Rev. Sci. Instrum. **77**, 041101 (2006).
17. L. V. Wang, "Tutorial on Photoacoustic Microscopy and Computed Tomography," IEEE J. Sel. Top. Quantum Electron. **14**(1), 171–179 (2008).
18. M. Pramanik and L. V. Wang, "Thermoacoustic and photoacoustic sensing of temperature," J. Biomed. Opt. **14**(5), 054024 (2009).
19. A. Danielli, K. Maslov, J. Xia, and L. V. Wang, "Wide range quantitative photoacoustic spectroscopy to measure non-linear optical absorption of hemoglobin," Proc. SPIE 8223, 1–6 (2012).
20. Y. Yamaoka and T. Takamatsu, "Enhancement of multiphoton excitation-induced photoacoustic signals by using gold nanoparticles surrounded by fluorescent dyes," Proc. SPIE 7177, 1–9 (2009).
21. M. Zhang, Z. Che, J. Chen, H. Zhao, L. Yang, Z. Zhong, and J. Lu, "Experimental determination of thermal conductivity of water-agar gel at Different concentrations and temperatures," J. Chem. Eng. Data **56**(4), 859–864 (2011).
22. D. Haemmerich, D. J. Schutt, I. dos Santos, J. G. Webster, and D. M. Mahvi, "Measurement of temperature-dependent specific heat of biological tissues," Physiol. Meas. **26**(1), 59–67 (2005).
23. Y. H. Lai, C. F. Chang, Y. H. Cheng, and C. K. Sun, "Two-photon photoacoustics ultrasound measurement by a loss modulation technique," Proc. SPIE 8581, 1–8 (2013).

1. Introduction

Traditional optical microscopy can easily achieve imaging with a spatial resolution up to the diffraction limit of light, but with a limited penetration depth. On the other hand, the medical ultrasonography has a high penetration depth over several centimeters, but the resolution is limited by the wavelength of sound. Therefore, how to combine light and sound together to achieve high-resolution and deep-tissue imaging becomes a challenging research topic during the past decade, especially for non-invasive diagnosis of various lesions, for the application of virtual biopsy, and for the application of functional tomography.

One of the innovations in the optical three-dimensionally (3D) imaging is the multi-photon fluorescence microscopy (MPFM), which uses a femtosecond near-infrared light source to achieve sub-micron resolution with a penetration depth deeper than that of the traditional confocal microscopy based on visible light. However, because the induced fluorescence suffers high attenuation caused by the tissue scattering and absorption, the record penetration depth is around 1 millimeter [1,2]. On the other hand, photo-acoustic tomography, which combines light and sound, enables penetration depth as deep as centimeters [3] with resolution limited by sound wavelengths. Because high frequency ultrasound has a high attenuation constant in tissues, the penetration depth would be reduced to the sub-millimeter region if the adopted acoustic wavelength was reduced to the micrometer scale [4,5]. Therefore, there is always a compromise between the spatial resolution, the contrast, and the penetration depth.

In order to achieve deep tissue imaging with a high optical resolution and an improved penetration depth compared with the current MPFM, multi-photon photoacoustic imaging is highly desired [6–11]. Similar to MPFM [12,13], the photo-excited acoustic signals should be generated nonlinearly by high-intensity optical fields within the focal volume, so the spatial (E.g. lateral and axial) resolution can be controlled by the optical point spread function, while the image would be acquired by scanning and mapping the laser beam within the tissues. Different from MPFM, to avoid the high attention of the weak fluorescence signals generated

#199491 - $15.00 USD Received 16 Oct 2013; revised 9 Dec 2013; accepted 9 Dec 2013; published 3 Jan 2014

deep inside the tissue, it is feasible to detect the two-photon-absorption-induced long-wavelength sound waves, of which the penetration depth is up to the centimeter scale.

Unfortunately, although different two-photon photoacoustic detection methods have been proposed, how to efficiently separate the multi-photon-absorption-induced acoustic signals from the single-photon-absorption-induced signals is still a critical issue [6,10,11,14,15], with the fact that the nonlinear signal is several orders of magnitude weaker than its linear counterpart. Furthermore, because the linear signal is generated within the whole light path where the excitation light passing through, it is thus impossible to distinguish whether the signal is generated only inside the focal volume, especially in an unknown material under test with a broadband response. This issue casts a shadow on the applicability of the previous works. To make the multi-photon photoacoustic microscopy feasible, the technique to be developed must achieve the nonlinear signal specificity inside the bio-tissues.

In this paper, we first present the measurement of the two-photon photoacoustic signals by the conventional amplitude-modulation-detection technique, and indicate the fundamental limitations of the technique. Then, we focus our attention on a loss modulation technique, and validate its detection capability to improve the frequency spectrum sensitivity and selectivity by several orders of magnitude, with examples of second harmonic generation and two-photon absorption measurements. After that, we discuss the enhancement of the two-photon photoacoustic signal by mixing the fluorescence dye with nanoparticles (dilute black carbon solution), and demonstrate the background-free nonlinear photoacoustic signal detection. Finally, we integrate the whole system with a raster scanner, and first demonstrate the femtosecond-laser-based two-photon photoacoustic imaging, with the abilities to remove the single-photon background, by optical scanning inside phantom tissues.

2. The existence of the two-photon photoacoustic signal

We started with a simple motivation to measure the absorption cross section of fluorescence dye and nano-particles in the aqueous solution. According to the thermal acoustic effect [16], materials can absorb light and convert the energy into mechanical vibrations. If light is periodically on and off, the material will be heated up by light excitation and be cooled down through the relaxation process. The periodic thermal expansion generates acoustic waves inside the material, and the efficiency is dominated by the absorption coefficient of light, the heat capacity, square of the speed of sound, and the thermal expansion coefficient of the materials.

We used a Ti: Sapphire femtosecond laser (Spectra Physics Tsunami, λ = 800nm, repetition rate = 80MHz) with a pulse width around 100fs (measured with an autocorrelator: AC-100 ps, UVisIR) and pulse energy of 2.06nJ to provide the pulse train excitation with high peak intensity and low pulse energy. An acoustic optical modulator (AOM; 23080-3-.85-LTD, Neos Technologies) operating in the normal mode was used as a chopper. A function generator was used to control the modulation depth and profile of the AOM, so the light output was intensity modulated. We also minimized the high harmonics by using a pure sinusoidal input generated by a function generator (33210A, Agilent). Then, an objective (SLMPlan 50X/0.45 15 mm WD, Olympus) with its back aperture filled focused the femtosecond laser pulse onto the sample, while Rayleigh criteria gives us an estimated focal beam waist of 0.92μm. After the sample cavity was a water cavity, and we used an immersion type ultrasonic transducer (V303, Olympus) to detect the ultrasound and transform it into electrical signals. With a lock-in detector (SR844, Stanford Research) we demodulated the electrical signals with the same frequency of the function generator, as depicted in Fig. 1.

#199491 - $15.00 USD Received 16 Oct 2013; revised 9 Dec 2013; accepted 9 Dec 2013; published 3 Jan 2014

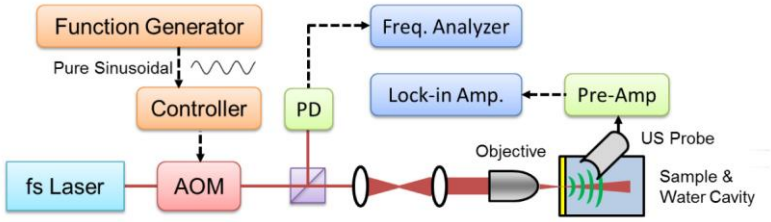

Fig. 1. The experimental design for testing the photo-acoustic phenomenon.

By measuring the ultrasonic signal intensity versus optical excitation power, as shown in Fig. 2(a), we could determine the source of the ultrasonic signal. The 20x diluted gold nanoparticles and the 20x diluted silver nanoparticles (PL-Au-S20-05mg and PL-Ag-S10-1mg, PlasmaChem) had strong single-photon absorption, whose power dependency was linear (~-20dB/OD). On the other hand, the 20x diluted fluorescence dyes (WKP1-Y and WKP1-P, which were extracted from highlighters (Zebra, Liberty Stationery Corp.) bought from a stationary store) exhibited strong two-photon absorption when the excitation power is high (with low OD), with a nonlinear power dependency of ~-40dB/OD. When the excitation power is low (with high OD), nonlinear absorption becomes weaker than the linear absorption and linear power dependency (~-20dB/OD) dominates again. Furthermore, we also conducted the experiment on pure diamond nano-particles (Institute of Atomic and Molecular Sciences, Academia Sinica, Taiwan), which showed almost no absorption.

This simple experiment indicates that the absorption mechanism strongly depends on the band structure and the resonance level of the material. The noble-metal nano-particles can absorb light easily, even though the optical wavelength might be far away from the plasmon resonance. On the other hand, the fluorescence dye has no electron-transition level near the excitation wavelength, so the transition can only occur through the two-photon absorption (2PA), which also induced strong two-photon fluorescence (2PF) during the experiment. If the bandgap is too large, no linear nor nonlinear absorption occurred. This experiment not only confirms the existence of the two-photon photoacoustic signal, but also indicates that the multi-photon photoacoustic phenomenon is not unusual in dyes.

We also analyzed the low-frequency optical spectrum of the incident beam. From Fig. 2(b), although our function generator sent a pure sinusoidal signal (f = 500.0kHz, harmonic to fundamental ratio (HFR) <-80dB) into the AOM, the imperfect temporal response of AOMs to external sinusoidal amplitude modulation induced linear (–20dB/OD) high harmonics in the modulated optical spectrum (HFR~-30dB). This induced a linear background in the high harmonic components. Under this circumstance, we could not distinguish linear and nonlinear absorption by detecting the high harmonics of the chopping frequency, because all high harmonics carried the same information as the fundamental frequency.

The main issue for the multi-photon photoacoustic detection is the relatively low nonlinear absorption cross section. Without a special detection design, the single-photon absorption signal can easily dominate over the multi-photon absorption signal, like the high OD case, so the source of the absorption is indistinguishable unless the power dependency experiment is performed. This becomes a fundamental constraint for designing the multi-photon photoacoustic microscope, since we cannot distinguish the nonlinear signal source in the bio-tissue when large linear background exists. The inevitable linear-photoacoustic background degrades the signal contrast and applicability of the previous nonlinear photoacoustic works [6,7,11].

Another important issue is that when laser light intensity is high, the local temperature change inside the sample would be a concern. In the case where the pulse width is within the thermal confinement time of an absorber, the pressure of an induced photoacoustic wave could be derived as a function dependent on the Gruneisen parameter (dimensionless), which is determined by the temperature of the absorber [17]. Since the instantaneous temperature increment from the femtosecond laser pulse heating has negligible effect on the Gruneisen

#199491 - $15.00 USD Received 16 Oct 2013; revised 9 Dec 2013; accepted 9 Dec 2013; published 3 Jan 2014

parameter, the parameter only depends on the base temperature of the absorber [18]. Therefore, the base temperature fluctuation (e.g., from heat accumulation due to continuous laser illumination) would possibly contribute nonlinearity to the measured photoacoustic signals [19]. However, in the power dependency experiment of photoacoustic signals, the sample cavity was bathed within a large amount of water, so it was hard for local heat accumulation to happen. As a result as being supported by experimental results and numerical calculations, there was no evidence to support the possible source of nonlinearity originated from the base temperature variation in our study (will be discussed in chapter 4 and 5). We therefore eliminate this effect due to negligible changes in the Gruneisen parameter.

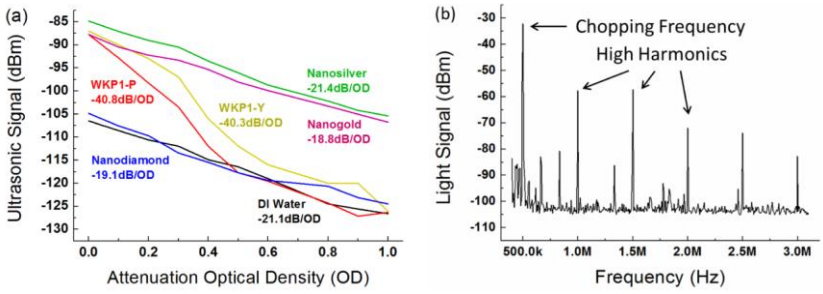

Fig. 2. (a) The power dependency experiment for different kinds of nano-particles and fluorescence dyes. Note that the fluorescence dyes had strong nonlinear absorption. The pulse energy was 2.06nJ/pulse. (b) The imperfect temporal response of the AOMs to the external sinusoidal amplitude modulation. The high harmonics existed and caused the linear background. The HFR was −30dB, and the power dependency of the high harmonics was linear. (−20dB/OD)

3. Loss modulation technique

To avoid the fundamental flaws of the AO modulation system, we focus our attention on a loss modulation technique [14]. This technique is a modification to a Michelson interferometer by installing two AOMs operating in the continuous mode in two arms of the interferometer. These two AOMs are with a difference in their modulation frequencies. The original laser beam is split into two sub-beams by the first beam splitter. Then, the two sub-beams will pass through different AOMs. When the two sub-beams are both spatially and temporally recombined via the second beam splitter, the frequency difference in modulation causes a beating. This results in a high-purity-sinusoidal waveform on the output beam envelope. If we assume the modulation frequencies of AOMs are f_1 and f_2 respectively, and the repetition rate of the femtosecond laser is f_R, then the first order beating frequency depends on the diffraction orders of the AOMs, n_1 and n_2, along with the multiple, n, of the repetition rate.

$$\Omega(f_1, f_2, f_R) = \min(|n_1 f_1 - n_2 f_2 + n f_R|) \quad (f_1 \sim f_2 \sim f_R >> \Omega,\ n_1, n_2, n \in \mathbb{Z}) \qquad (1)$$

When the combined collinear incident light (λ_R = 800nm) passes through a barium borate (BBO) crystal for second harmonic generation (λ_B = 400nm), or when the photo-detector (DET-200, Thorlabs) has two-photon absorption, such nonlinearities generate the second order beating, and cause the beating frequency exactly doubled. The schematic diagram of the loss modulation technique as well as a test for the second harmonic generation is shown in Fig. 3, and the beating effect in frequency is illustrated in Fig. 4. In this article, we used two AOMs with modulation frequency of 80.5MHz (f_1) and 81MHz (f_2) for our loss modulation technique, and both AOMs are in the first diffraction order. A spectrum analyzer (E4402B, Agilent) was used to detect the radio-frequency (RF) spectra of the photo-detector without electronic bias or amplification. As the experiment spectra shown (see Figs. 5(a)-5(c)), the 1st order beating generated one pair of sidebands besides the repetition rate peak, and the 2nd order beating generated two pairs of sidebands. In addition, the frequency separation between

#199491 - $15.00 USD Received 16 Oct 2013; revised 9 Dec 2013; accepted 9 Dec 2013; published 3 Jan 2014

each peak was exactly equal to $\Omega(f_1, f_2, f_R)$. We could see that the loss modulation technique imposed a pure sinusoidal modulation on the incident light, which had no high harmonic component (SNR>50dB), as shown in Fig. 5(d) and being discussed below.

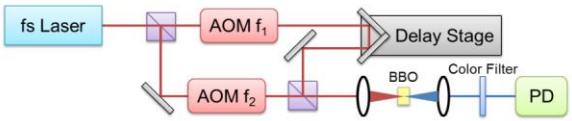

Fig. 3. Schematic diagram showing the basic experiment setup to test the loss modulation technique. For the infrared light experiment, the BBO crystal was removed. For the blue light experiment, we used color filters to remove the infrared light.

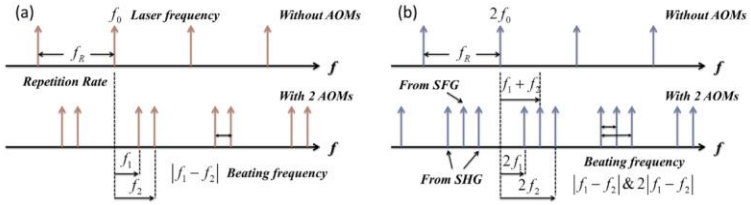

Fig. 4. (a) The collinear NIR light beats with itself if its components have different frequency shifts provided by AOMs. (b) When the collinear NIR light passes through the BBO crystal, the collinear light creates sum frequency generation (SFG) and second harmonic generation (SHG). The blue light creates 1st order beating and 2nd order beating on itself.

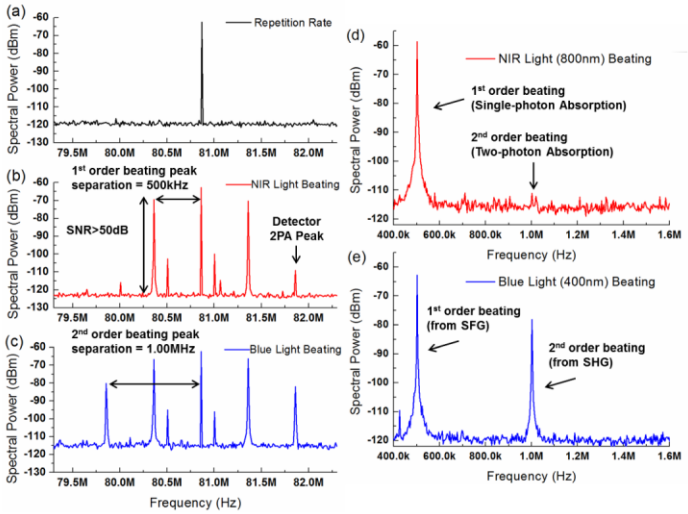

Fig. 5. (a) The original repetition rate of the femtosecond laser (b) The first order beating spectrum (c) The second order beating spectrum (d) The low frequency spectrum of the collinear NIR light (λ_R = 800nm) (e) The blue light generated by BBO (λ_B = 400nm). Note that the frequency separation is related to the diffraction order of the beam, the modulation frequency of AOMs, and the laser repetition rate. Moreover, the 2nd order beating peak originates from the nonlinearity of the sample or of the detector.

In Fig. 5(d) and 5(e), we examined the RF spectra of the photodetector illuminated by the combined collinear incident light (λ_R = 800nm) and second harmonic generated light (λ_B = 400nm), respectively. For the 800nm light, we observed the expected beating peak of 500kHz (1st order beating) and an unexpected tiny signal located at the position of the 2nd order beating. This unexpected beating could be due to imperfect sinusoidal modulation or due to the two-photon absorption of the photodetector to the incident light. For 400 nm light, we

#199491 - $15.00 USD Received 16 Oct 2013; revised 9 Dec 2013; accepted 9 Dec 2013; published 3 Jan 2014

successfully observed the both the 1st and the 2nd order beatings, with a strong 2nd order beating generated due to the second harmonic generation (SHG) nonlinearity. With no other high harmonics, the result of 400 nm light was consistent with the theoretical derivation.

To further investigate the origins of various signals, we conducted the power dependency measurement on the 1st and the 2nd order beating. Figure 6 shows the experimental results. For 800nm light as shown in Fig. 6(a), the 1st order beating possesses an expected linear dependency (~-20dB/OD) with the incident power, while the 2nd order beating possesses square dependency (~-40dB/OD) with the incident power, supporting the SHG nature of the observed 2nd order beating. For 400nm light as shown in Fig. 6(b), both 1st and 2nd order beatings possess an expected square dependency (~-40dB/OD) with the incident 800nm power and an expected linear dependency (~-20dB/OD) with the doubled 400nm power. Combining Fig. 5 with Fig. 6, we could confirm that 1) the adopted loss modulation technique does impose a pure sinusoidal modulation on the incident light, which has no high harmonic component (SNR>50dB), and 2) SHG appears as 2nd beating and is with a quadratic dependency on incident light power.

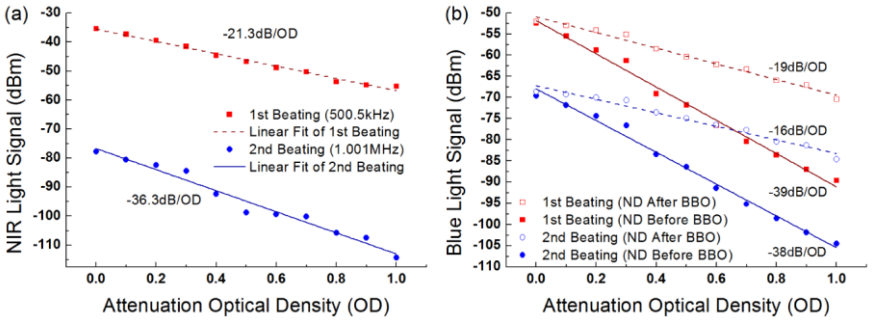

Fig. 6. (a) The NIR light (λ_R = 800nm) power dependency with 0.5mW incident power. The two-photon absorption is quadratically dependent on the incident power. (b) The blue light (λ_B = 400nm) power dependency with 0.2mW incident power. Note that both the 1st and 2nd beating signals are generated by BBO, so they have the same power dependency. (ND: Neutral Density filter)

Since the loss modulation technique provides pure sinusoidal modulation, and high RF harmonics can only be generated by the nonlinear phenomena, it becomes an excellent tool to study the nonlinear response of a material. In addition, because the femtosecond laser provides high repetition rate excitation, the transient response of the material is no longer dominant. That is, the high repetition rate laser (~80MHz) induces the narrowband excitation of the material, and suppresses the wide band transient spectrum, as compared to the traditional low repetition rate (<kHz) nanosecond laser. This concept could be clearly illustrated in Fig. 7. Furthermore, the beating frequency only depends on the modulation frequency of AOMs and the repetition rate of the femtosecond laser, so we can adjust the beating frequency by changing the diffraction order or the modulation frequency of AOMs. In sum, we verify the spectrum sensitivity and selectivity of the loss modulation technique.

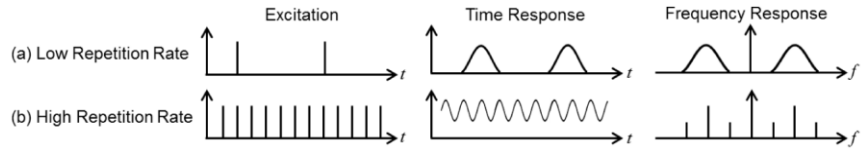

Fig. 7. Lasers with different repetition rate induce different system responses. (a) The low repetition rate laser excites the system with observable transient response, which is equivalent to the broad band response in the frequency domain. (b) The high repetition rate laser excites the system by forced resonance, so only the frequencies equal to the multiple of the repetition rate can be excited. The response spectrum becomes discrete, which is equivalent to the narrow band response if we detect the response at a specific frequency.

#199491 - $15.00 USD Received 16 Oct 2013; revised 9 Dec 2013; accepted 9 Dec 2013; published 3 Jan 2014

Finally, it is worthwhile to discuss the limitation of the loss modulation technique. Since the frequency spacing within the laser frequency comb is equal to the repetition rate (80MHz in this case), according to the Nyquist-Shannon sampling theorem, the maximum modulation frequency cannot exceed $f_R/2$. This restricts our maximum 1st order beating frequency to be $f_R/4$, which is one half of the 2nd order beating frequency. For a conventional commercial femtosecond laser, the maximum 1st order beating frequency is around 20MHz.

4. The enhancement and the selective detection of the two-photon photoacoustic ultrasound

From the above discussion, we can see clearly the advantage of detecting the photo-acoustic signal using the loss modulation technique. Theoretically speaking, because water has a small thermal expansion coefficient and a large specific heat, the thermal confinement condition and stress confinement condition [16] make it hard to detect the multi-photon photoacoustic signal, especially for the high-repetition-rate femtosecond laser, whose pulse energy is only 1nJ~20nJ/pulse. Moreover, since the linear absorption and the nonlinear absorption coexist in a system, and the linear signal is several orders of magnitude higher than the nonlinear one, both signals will interfere with each other and cannot be separated by traditional time domain detection. How to enhance the weak nonlinear signal and distinguish it from the linear signal background becomes a critical issue for the applicability of the multi-photon photoacoustic microscopy.

In order to enhance the multi-photon photoacoustic signal, mixing the fluorescence dye with other nano-particles has been proposed [20]. In our experiment, we mixed the fluorescence dye, which exhibits strong two-photon fluorescence (WKP1-Y), with dilute carbon solution (Wu-Zhu Calligraphy Paints). The mechanism is concisely shown in Fig. 8. Because the carbon particles capture the fluorescence dye and carbon particles have a wide energy-band structure, the particles become an intermediary agent to transfer the two-photon fluorescence into two-photon photoacoustic ultrasound. When the incident light induces the two-photon absorption of the fluorescence dye, some of the energy transferred into fluorescence, while the rest of energy, with the help of energy levels of carbon particles, transferred into phonon vibration. By this way, we can generate the two-photon photoacoustic ultrasound more efficiently.

Besides, in the previous section, we verify the validity of the loss modulation technique, so we can apply the technique to the ultrasound system. That is, if we can detect the 2nd order beating by using an acoustic transducer and the measured power dependency curve is quadratic, then we can conclude that such a signal is generated through the nonlinear absorption. In general, once we detect the 2nd order acoustic beating, we can attribute it to the background-free 2PA photoacoustic signal.

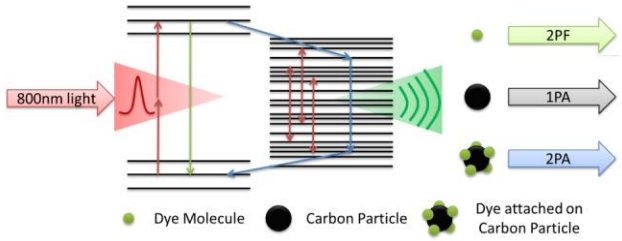

Fig. 8. The enhancement mechanism of the two-photon photoacoustic signal by mixing carbon particles and fluorescence dyes. The energy transfers from 2PF into 2PA with the help of carbon particles. This phenomenon is similar to fluorescence resonance energy transfer (FRET).

Figure 9(a) shows our overall experimental setup. We used the immersion-type ultrasonic probe (V303, Olympus) with spherical focus (f = 15mm) to increase the acoustic numerical aperture (NA). Besides, we used an ultra-low noise preamplifier (Ultrasonic Preamp 5660B, Olympus) with flat gain of 40dB from 20kHz to 2MHz, so we prevented the nonlinearity of

#199491 - $15.00 USD Received 16 Oct 2013; revised 9 Dec 2013; accepted 9 Dec 2013; published 3 Jan 2014

the electronic system. The femtosecond NIR light was focused at the bottom of the designed cavity (see Fig. 9(b)) by a long working distance objective (SLMPlan 50X/0.45 15 mm WD, Olympus). We also used concentrated fluorescence dyes with 4000x diluted carbon solution mixture, so that the excitation light could not penetrate through the cavity, and we therefore avoided the direct light incidence on the probe. The frequency analyzer recorded thus measured RF spectra, and the lock-in amplifier recorded the measured signal for power-dependency studies.

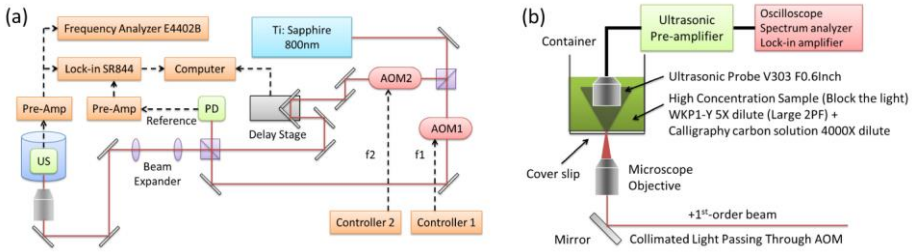

Fig. 9. (a) The experiment setup. (b) The design of the optical cavity. Since the concentration of the solution is very high, the light cannot penetrate. Therefore, we prevent the direct incidence of the laser beam on the ultrasonic probe.

We first tested the solution of mere 4000x diluted carbon solution under the same condition. Shown as the red curve plotted in Fig. 10(a), we did not observe 2nd order beating signal around 1MHz, indicating 1) insignificant 2PA in diluted carbon solution, 2) the pure sinusoidal modulation on the incident light with no high harmonic component (SNR>50dB), and 3) negligible changes in the Gruneisen parameter generating the nonlinear signal. In contrast, when testing the mixture with fluorescence dyes, shown as the black curve in Fig. 10(a), we found that the single-photon and two-photon photoacoustic signals coexisted in the cavity. We thus conclude that the measured 2nd order beating signal at 1MHz contributed from the 2PA signal, while the single-photon photoacoustic signal was 60dB (1000 times) larger than the two-photon photoacoustic signal. Further supported by the measured power dependency (see Fig. 10(b)), we confirm that the 1st order beating signal is linearly proportional to the incident light power, an indication of linear absorption, while the 2nd order beating depends quadratically on the incident power, an indication of two-photon absorption. Therefore, we successfully demonstrated that by detecting the 2nd order beating we can successfully separate the two-photon photoacoustic signal from the single-photon photoacoustic one.

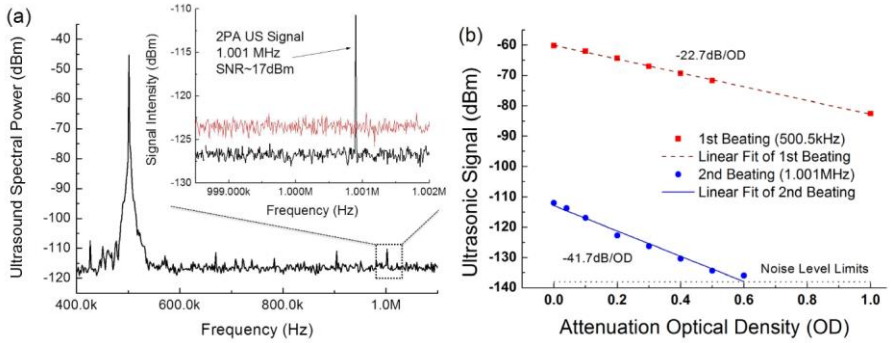

Fig. 10. (a) The existence of the 2nd order beating signal in the dye-carbon mixture. This peak vanishes if we only use pure dilute carbon solution, shown as the red curve in the enlarged spectrum. (b) The power dependency of the 2nd order beating (2PA US) is quadratic. The laser pulse energy is 9.34nJ/pulse with a repetition rate of 80.305MHz.

#199491 - $15.00 USD Received 16 Oct 2013; revised 9 Dec 2013; accepted 9 Dec 2013; published 3 Jan 2014

5. Application–nonlinear photoacoustic microscopy

In order to demonstrate the applicability of the loss modulation technique in nonlinear photoacoustic microscopy, we set our sample cavity on a motorized 3D translational stage for raster scanning. Although raster scanning limited our scanning time to be more than 100 seconds per image, our main point is to demonstrate the feasibility of the background-free nonlinear photoacoustic microscopy with the loss modulation technique. Currently, the sampling rate of the pixels was 64Hz, limited by the raster scanning system, and the integration time of the lock-in detector was 10ms. For a 100 pixels by 100 pixels image, it took 3 minutes for one 2D scanning. For future application with the 1MHz acoustic frequency, the sampling rate of the lock-in detector can achieve 100kHz with a 0.4 frames/second imaging speed for 512 pixels by 512 pixels images after combined with a galvo scanner. For even higher frame rate, high-speed digital signal processing or higher beating frequency has to be adopted.

We used agar jelly (2.5~4wt%) as our phantom tissue. Since we want to demonstrate laser-scanning imaging, we produced some small donut shape patterns (3mm thick) filled with contrast agents (a mixture of 5x diluted WKP1-Y solution and 4000x diluted carbon solution), by the capillary tube (with 1.5mm inner diameter and 1.8mm outer diameter) at the bottom of the sample cavity. The pattern dimension is similar to the ultrasonic wavelength (λ_{US} = 1.5mm at 1MHz). On the other hand, to verify that the technique can achieve ultrasonic collection depth, we put another thick agar jelly (7mm) on the top of the original pattern. Figures 11(a) and 11(b) show the photos of our homemade sample. The strong scattering of the agar layer prevented the ultrasonic probe from the light incidence. Therefore, the light signal wouldn't interfere with the ultrasonic signal. During the experiment, we filled the cavity with deionized water and immersed the ultrasonic probe in the water without direct contact with the agar layer. Because the agar jelly had similar thermal conductivity and heat capacity to that of water [21,22], by simple calculation, it would take more than 10 minutes for the overall sample temperature to rise by 1 degree even if all the laser light energy was absorbed and became heat. Combining our previous experimental result with this calculation, we believe that the base temperature of the sample did not change much when imaging, thereby eliminating the effect from the varied Gruneisen parameter on the 2nd order beating signals.

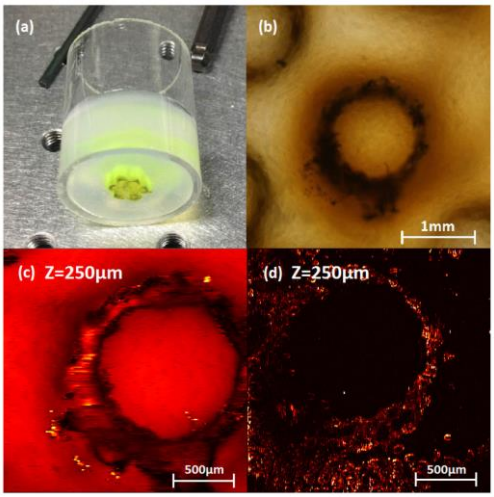

Fig. 11. (a) The cavity, the pattern and the phantom design (3mm agar pattern with 7mm thick agar layer) (b) The image of the pattern under the microscope (c) The single-photon photoacoustic image. The large background signal reduces the contrast ratio of the image, so the edge is blurred. (d) The two-photon photoacoustic image (depth z = 250μm). The signal only exists with the presence of the contrast agent, so the edge of the pattern is sharp. The pulse energy is 5.6nJ/pulse.

#199491 - $15.00 USD Received 16 Oct 2013; revised 9 Dec 2013; accepted 9 Dec 2013; published 3 Jan 2014

To our surprise, the experiment result was beyond our expectation. Our system could both record the 1st order beating, which generates the single-photon photoacoustic image (see Fig. 11(c)), and the 2nd order beating, which generates the two-photon photoacoustic image (see Fig. 11(d)). Since our method detected the photoacoustic signal in the frequency domain, and all light paths generated single-photon photoacoustic signal due to the linear light absorption of the agar, we actually got a time-averaged single-photon acoustic image with blurred edge contrast of the pattern. One sees that in the single-photon photoacoustic image, due to a lack of spatial filtering or temporal resolving mean, contribution of the induced linear photoacoustic signals within the entire light cone are integrated inevitably into the corresponding pixel. That is to say, strong signals due to linear absorption are homogeneously observed in our sample. However, this was not the case for the two-photon photoacoustic image. Only when the contrast agent contributes 2PA inside the focal volume, could the 2nd order beating signal exist. Therefore, we could image the detailed structure of the pattern by laser scanning with a high contrast ratio and with a 250μm-depth inside the phantom sample.

We also tried to conduct the experiment on real biological tissues. First, we dyed a piece of leaf tissue (Centipede Tongavine, or Epipremnum pinnatum for the scientific name) with the same contrast agent as that in the homemade sample case, and examined the tissue under a microscope (see Fig. 12(a)). Then, we buried the leaf tissue beneath the agar phantom, with a 1mm-thick agar layer between the leaf tissue and the bottom of the cavity. We put a 10mm-thick agar layer above the leaf tissue, so the light could not penetrate through the phantom.

By recording the 2nd order beating signal, we could image the tissue boundary with a high contrast ratio. The two-photon photoacoustic image is shown in Fig. 12(b). The cell wall absorbed most of the contrast agent, so it generated a large two-photon photoacoustic signal. With the help of the lipid, the contrast agent could be ingested into the cell, so we could image the inner structure of the cell also. According to our image, the lateral resolution underneath a 1mm-thick agar phantom was approximately 10μm, due to the degradation of the point spread function by the strong scattering in the agar phantom. With an acoustic wavelength of 1.5 mm, this two-photon photoacoustic image showed that the resolution was determined by the optical focusing.

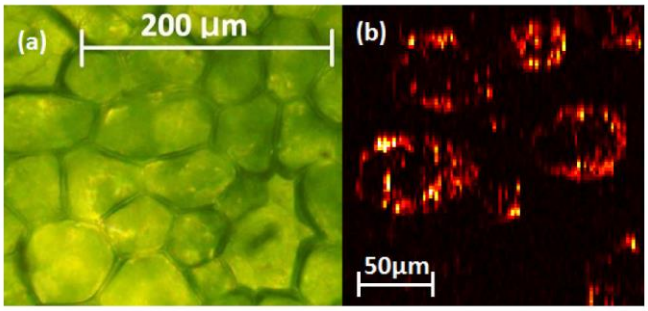

Fig. 12. (a) The image of the leaf tissue under the microscope. (b) The two-photon photoacoustic image of the leaf tissue underneath 1mm-thick phantom. The image shows the application of the two-photon photoacoustic imaging on a biological tissue. The strong scattering in the agar phantom degraded the lateral resolution to approximately 10μm. The pulse energy is 2.8nJ/pulse.

6. Conclusion

In summary, we showed the existence of the two-photon photoacoustic signal in the fluorescence dye. Then, we investigated the loss modulation technique for its frequency selectivity and sensitivity, and we used the technique to separate the two-photon photoacoustic signal from the single-photon photoacoustic signal. In addition, we found that the mixture of the fluorescence dye and dilute carbon solution could be used as a contrast agent in the two-photon photoacoustic imaging. Finally, based on our finding, we proposed a prototype of the background-free nonlinear photoacoustic microscope and demonstrated

#199491 - $15.00 USD Received 16 Oct 2013; revised 9 Dec 2013; accepted 9 Dec 2013; published 3 Jan 2014

background-free optical scanning bio-imaging underneath 1mm-thick phantom tissues with an optical spatial resolution.

Acknowledgments

This work is funded by National Science Council, Taiwan (NSC 100-2120-M-002-009) and National Health Research Institute (NHRI-EX101-9936EI). We appreciate the support of Prof. Pai-Chi Li, whose group inspired us to design a better ultrasonic cavity and testing system. We thank Dr. Huan-Cheng Chang, whose group provided us with the sample of pure nano-diamonds. We acknowledge the valuable technical supports from Dr. Chien-Cheng Chen and Dr. Pierre-Adrien Mante. We appreciate the useful advices and generous discussions from Dr. Yu-Ru Huang and Dr. Ming-Rung Tsai. All the works were performed in National Taiwan University. This work is based on a previous SPIE conference proceeding [23]. The content is fully expanded, developed, reorganized and corrected.